Differences between morphological and electrophysiological retinal ganglion cell classes

Syeda Zehra[1], Damien G. Hicks[1,2], Alex Hadjinicolaou[3,4], Michael R. Ibbotson[3,5], Tatiana Kameneva[1,6]

Abstract— **Retinal prostheses work by delivering electrical pulses to the surviving retinal neurons. A pattern of electrical stimulation can generate a perception of vision in blind patients. To improve efficacy of retinal implants, it is important to understand how different classes of retinal neurons respond to electrical stimulation and if a classification can be made based on the electrophysiological properties of neurons. We use previously recorded patch clamp data from retinal ganglion cells classified into morphological classes (A, B, C, D) and functional types (ON, OFF, ON-OFF). We use a machine learning technique to separate data based on the recorded electrophysiological parameters. Results show that the clusters discovered using the machine learning technique do not correspond to the morphological or functional classes used by neuroscientists.**

Introduction

Age-related macular degeneration (AMD) and retinitis pigmentosa (RP) are medical conditions that lead to the loss of light-sensitive cells in the retina. In these conditions, due to the atrophy of cells that convert light energy into electrochemical signals, visual information cannot be transmitted to the visual cortex. The later stages of these diseases cause blindness. In people with AMD and RP a large number of retinal neurons survive the loss of light-sensitive cells [6].

Retinal prostheses deliver patterns of electrical stimulation through an array of electrodes that generate activity in retinal neurons, and ultimately generate visual perception [9], [10]. Electrical stimulation of the retina generates a perception of spots of light called phosphenes. A mosaic of phosphenes may be used to form a two-dimensional image. To improve efficacy of retinal prostheses, it is important to understand responses of different classes of retinal neurons to electrical stimulation.

Retinal ganglion cells (RGCs) are the output neurons of the retina that carry visual information via the optic nerve to the brain. RGC responses to electrical stimulation have been studied in [3], [4], [8]. There are more than 15 different morphological classes of RGCs in the mammalian retina; however their functional role is not completely understood [11]. It is unclear if each cell type encodes a different aspect of the visual scene transmitted to the brain in parallel. Recently, it has been shown that there may be more than 30 functional output channels in the mouse retina [1]. Classification of RGC types is controversial and is the basis of a heated debate [1].

[1] Faculty of Science, Engineering and Technology, Swinburne University, Australia. [2] Centre for Micro-Photonics, Swinburne University Australia. [3] National Vision Research Institute, Australian College of Optometry, Australia. [4] Harvard Medical School, Boston, USA. [5] Department of Optometry and Vision Sciences, University of Melbourne, Australia. [6] Department of Biomedical Engineering, The University of Melbourne, Australia. Contact: Tatiana Kameneva, tkameneva@swin.edu.au

There are two parallel pathways from the retina to the visual cortex: ON and OFF pathways. ON RGCs respond with increases in the spike rate when a spot of light is illuminated in the center of their receptive fields. OFF cells respond in the opposite fashion; their spike rate is decreased at light onset and is increased at light offset. ON-OFF RGC types respond to both, light onset and light offset. There exists evidence that ON, OFF and ON-OFF cells have different intrinsic electrophysiology [7]. These cell types have different functional roles; however, with electrical stimulation, they are stimulated simultaneously which is unnatural for visual perception.

In this paper, we use machine learning techniques to divide previously recorded *in vitro* data into clusters. We analyze if the clusters discovered using the machine learning technique correspond to the morphological (A, B, D) or functional (ON, OFF, ON-OFF) classes used by neuroscientists. Understanding differences in electrophysiological properties between cell types may have important implications for the development of stimulation strategies for visual prostheses.

Methods

Morphology

We have used patch clamp data previously collected in our lab [5]. In short, data was collected from retinas of 6-11 month old Long Evans rats. Cells were classified into morphological classes (A, C, and D) using 3D reconstruction with a confocal microscope (Zeiss PASCAL), according to widely used criteria [11]. Only cells for which morphological classification could be reliably confirmed were used for the analysis. Different types were combined into one class for cluster analysis (i.e. A1, A2i, A2o were combined into A class, D1 and D2 were combined into D class). RGCs were classified into ON (i, inner), OFF (o, outer), and ON-OFF (D cells) types based on their dendritic stratification in the inner plexiform layer.

Recordings from 46 RGCs were used for the analysis presented in this paper, with the following distribution between classes: 17 cells from A class, 11 cells from C class and 18 cells from D class. No data from B class were used for analysis due to the small sample of recorded cells from this class. 6 cells were classified as ON types (inner), 16 as OFF type (outer) and 17 as ON-OFF type (directionally selective D cells).

Electrophysiology

For each cell, the following intrinsic electrophysiological parameters were measured: resting membrane potential, V_{rest}; frequency adaptation index, F_A; spike width, SW; input resistance, R_N; and sag value S, a measure of the

978-1-5386-3646-6/18/$31.00 ©2018 IEEE

rectification voltage of the membrane potential towards V_{rest}. The frequency adaptation index was calculated as $F_A = (f_{\max} - f_{\text{ss}})/f_{\max}$, where f_{ss} is the steady-state firing rate and $f_{\max}$ the maximum firing rate during the application of the 400 ms depolarization pulse, for details see [5]. Only cells for which all five electrophysiological parameters were recorded were used for analysis.

Cluster analysis

To analyze if the clusters found by a computational algorithm correspond to the morphological classes of the RGCs or functional cell types, the k-means algorithm was used to classify experimental data [2]. All experimental recordings (n=46) were used as an input into the algorithm. The number of clusters in the algorithm was chosen to be the same as the number of morphological classes (A, C, and D), $k = 3$. To avoid skewed results due to a dominating parameter (for example, very large value of the input resistance compared to the spike width), each measurement was standardized across samples to allow comparison of the relative variation of each parameter:

$$z_i = \frac{x_i - \mu_x}{\sigma_x},$$

where z_i is the normalized value corresponding to the measured electrophysiological parameter x_i; μ_x and σ_x are the mean and standard deviation for each measured electrophysiological parameter V_{rest}, F_A, SW, R_N, and S. For example, all recordings for V_{rest} were standardized based on the mean and standard deviation for V_{rest}. The objective of the k-cluster algorithm is to partition the experimental data $x = \{x_1, x_2, ..., x_N\}$ into three clusters $C = \{C_1, C_2, C_3\}$ so that the within-cluster sum of squares is minimal. N is the number of experimental observations. The objective function is to find the cluster assignment for each cell such that

$$\arg\min_{C} \sum_{j=1}^{3} \sum_{x \in C_j} ||x - \mu_j||^2 = \arg\min_{C} \sum_{j=1}^{3} |C_j| var(C_j)$$

The analysis was performed using MATLAB. To avoid confusion, the following terminology is used throughout the paper:

- Morphological classes: A, C, and D.
- Functional types: ON, OFF, and ON-OFF.
- Electrophysiological parameters: V_{rest}, F_A, S_W, R_N and S.
- Clusters: new groups separated by the electrophysiological properties found using the k-means algorithm.

RESULTS

Original morphological classes and functional types

First, we studied if the original morphological classes are evident in a 1-dimensional space for the electrophysiological parameters. A box plot of electrophysiological parameters recorded experimentally for each class is shown in Figure 1. Figure 1 illustrates that classes A, C, and D overlap in the ranges for the resting membrane potential V_{rest}, frequency adaptation index F_A, spike width SW, and sag S values. In R_N, the three cell classes cover different ranges suggesting the classes may be separated based on

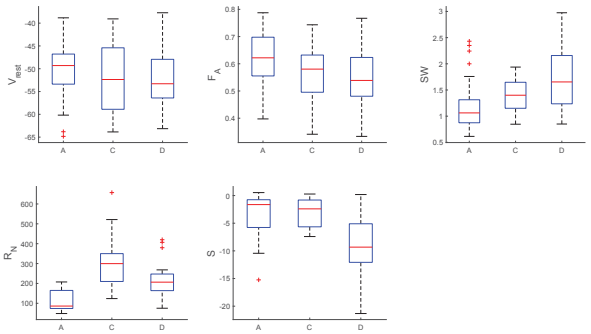

Fig. 1. Boxplots showing the distribution of the experimentally recorded intrinsic electrophysiological properties of RGCs, used for analysis. The red lines indicate the median; the bottom and top edges of each box indicate the 25th and 75th percentiles, respectively. The plus symbols show outliers. The whiskers extend to the most extreme data points not considered as outliers. Measured units: resting membrane potential V_{rest} [mV], frequency adaptation index F_A [-], spike width S_W [ms], input resistance R_N [MΩ], sag S [mV]. The same units are used in Figs. 2-5.

the input resistance. This is not surprising since one of the morphological properties (the cell's size) is reflected in the input resistance. For better visualization of the original morphological classes based on each cell's electrophysiological properties, we plot the original classes in 2-dimensional plots. Given five electrophysiological parameters, there exist $5 * (5-1)/2$ combinations of pairs. Figure 2 shows the original morphological classes in 2-dimensional plots. Class A has a small variation in the range of R_N values. Class A (grey circles) can be seen separately from other classes when R_N is plotted on one of the axes. Class C (pink triangles) has a tight cluster in the range of sag values, S. The same class of cells somewhat cluster together in the R_N vs S plot and in the S vs SW plot, indicating that there may be a parameter separation in the $R_N - S - SW$ space. However, overall the data from the three morphological classes are scattered across electrophysiological parameters and no clear clusters are observed.

Then, we investigated if the ON, OFF and ON-OFF cell types can be separated by their intrinsic electrophysiological parameters. The original data is plotted in Figure 3. There is a small separation between three types in the R_N vs S plot and in the SW vs S plot. This indicates that there may exist a manifold separating ON, OFF and ON-OFF cell types in the $R_N - S - SW$ space, similar to the morphological classes. This is difficult to see in two-dimensional plots. When ON and OFF RGCs (grey and orange symbols) are considered as one class, there is a clear separation of these cells from the ON-OFF type (pink triangles). For example, in the S vs S_W, S vs V_{rest}, R_N vs S, and S_W vs F_A plots. This supports previously published data that ON, OFF and ON-OFF types have different intrinsic electrophysiological properties [7].

New clusters found by the k-means algorithm

Figure 4 illustrates new clusters identified by the k-means algorithm based on the search to separate data on the differences in the electrophysiological parameters. Standardized

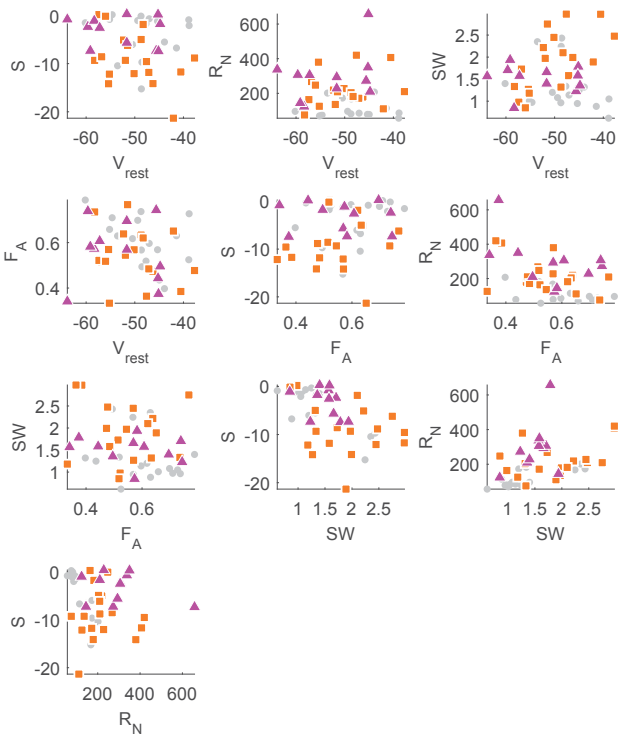

Fig. 2. Distribution of the original morphological cell classes. Class A: grey circles; Class C: pink triangles; Class D: orange squares.

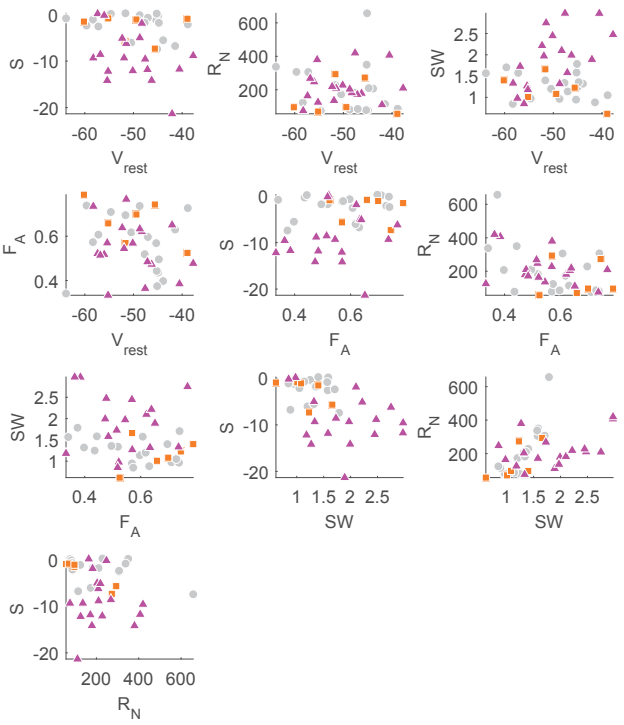

Fig. 3. Distribution of the original functional cell types. ON RGC type: orange squares; OFF type: grey circles; ON-OFF type: pink triangles.

measured parameters used for clustering were converted back to the original values when plotting. There is still some overlap between clusters because five-dimensional data is presented using 2-dimensional plots; however, there is clear separation in the the SW vs F_A and S vs SW plots. Results show that there is a different way to separate data; new clusters in Figure 4 do not correspond to morphological classes in Figure 2. This is indicated in Table 1 which shows the distribution of cells in each cluster. The majority of cells in Cluster 1 are Class A cells (54%). Cluster 2 has mixed cell classes (57% from Class C). Cluster 3 comprises of 71% Class D cells.

Table 1. Distribution of cell classes in each cluster.

	Class A	Class C	Class D
Cluster 1	13	6	5
Cluster 2	1	4	3
Cluster 3	3	1	10

Figure 5 illustrates clusters found by the k-means algorithm using only data for ON, OFF and ON-OFF cells. Note, there are some cells, for example A1 type, that are not identified as ON, OFF or ON-OFF types. These cells were excluded from the analysis presented in Figure 5 and Table 2. There is a clear separation into clusters in several plots, including S vs V_{rest}, SW vs F_A, R_N vs SW, and S vs R_N. Results show that the best way to separate data into clusters is based on the cell differences in the values for sag, resting membrane potential, spike width, and the cell's input resistance. Most cells in Cluster 2 were OFF type cells (75%), most cells in Cluster 1 were directionally selective ON-OFF RGCs (65%). It is difficult to make conclusions about ON-type cells due to the small sample size.

Table 2. Distribution of cell types in each cluster.

	ON cells	OFF cells	ON-OFF cells
Cluster 1	2	3	11
Cluster 2	4	12	3
Cluster 3	0	1	3

Conclusion and Discussion

Results show that the electrophysiological clusters found using a machine learning technique do not correspond to the morphological classes used by neuroscientists. Results show that the best way to separate data based on the electrophysiological properties is in the input resistance - spike width - sag space. We found that when only the ON, OFF and ON-OFF cells are considered for clustering, there is a clear separation of data in many parameters, including the cell's input resistance, sag, frequency adaptation index and spike width.

It is unclear if the cells from one cluster have a unifying functional role. This is left to explore in future work. Functional diversity of RGCs is discussed in [1]. Using two-photon calcium imaging, Baden et al (2016) discovered several new RGC types and show that there may be more than 30 functional cell types in the mouse retina, and possibly

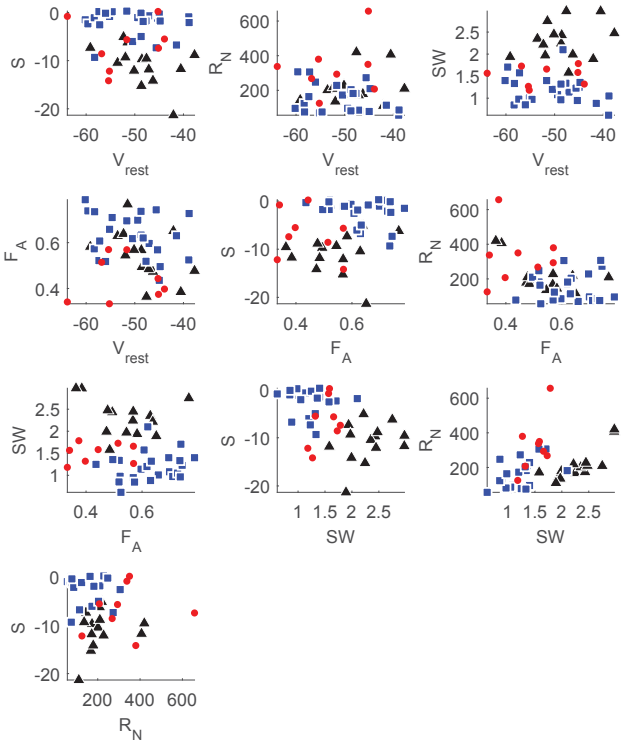

Fig. 4. Distribution of all cells in the new clusters. Clusters 1: blue squares, Cluster 2: red circles; Cluster 3: black triangles.

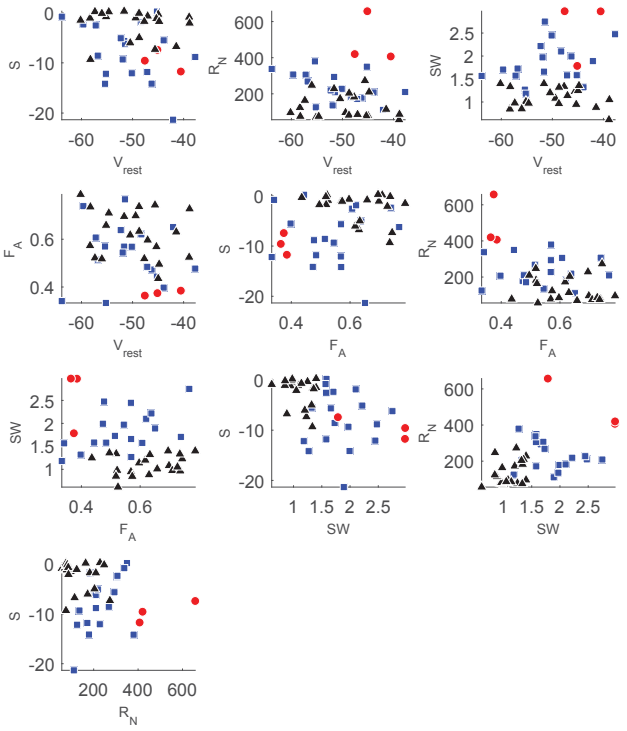

Fig. 5. Distribution of ON, OFF, ON-OFF cells in the new clusters. Clusters 1: blue squares, Cluster 2: red circles; Cluster 3: black triangles.

further subdivision is needed. In our work, we conservatively set the number of clusters to three. Our choice was based on the fact that we used *in vitro* data classified into three morphological classes and three functional types. In addition, it is easier to find a stimulation strategy that differentially stimulates three different groups of cells than a stimulation strategy for 30 different groups.

The best separation into clusters was seen when only ON, OFF and ON-OFF cell types were considered. It may be possible to differentially stimulate cell clusters based on their difference in the intrinsic electrophysiology. These results may have implications for stimulation strategies in visual prostheses.

One of the parameters that best separates clusters was the adaptation index, F_A. The cell's maximum and steady-state firing rates are reflected in this index. Variability in response to high rates of electric stimulation was found between different RGCs types [3]. It is reasonable to assume that the adaptation index is different for different cell types discussed in [3]. It is left for future work to investigate if cells in different clusters respond differently to high frequency stimulation.

Acknowledgments

TK acknowledges support through the Australian Research Council (ARC) Discovery Projects funding scheme (DP140104533). DGH was supported in part by ARC grant FT140101104. This research was supported by the ARC through the Centre of Excellence for Integrative Brain Function (CE140100007).

References

[1] T. Baden, P. Berens, K. Franke, M. R. Roson, M. Bethge, T. Euler. The functional diversity of retinal ganglion cells in the mouse.*Nature,* 529: 345350, 2016.

[2] C.M. Bishop. Pattern recognition and machiche learning, Springer, 738p., 2006.

[3] C. Cai, Q. Ren, N.J. Desai, J.F. Rizzo III, S.I. Fried. Response variability to high rates of electric stimulation in retinal ganglion cells. *J Neurophysiol,* 106: 15362, 2011.

[4] R.J. Jensen, J.F. Rizzo III. Responses of ganglion cells to repetitive electrical stimulation of the retina. *J of Neural Eng,* 4(1), S1, 2007.

[5] A.E. Hadjinicolaou, S.L. Cloherty, Y-S. Hung, T. Kameneva, M.R. Ibbotson. Frequency responses of rat retinal ganglion cells. *PLOS One*, 11(6): e0157676, 2016.

[6] R. Margalit et al. Retinal prosthesis for the blind. *Survey Ophtalm,* 47(4): 335 - 356, 2002.

[7] D.J. Margolis, P.B. Detwiler. Different mechanisms generate maintained activity in ON and OFF retinal ganglion cells. *J Neurosci,* 27(22), 59946005, 2007.

[8] M.I. Maturana, N.V. Apollo, A.E. Hadjinicolaou, D.J. Garrett, S.L. Cloherty, T. Kameneva, D.B. Grayden, M.R. Ibbotson, H. Meffin. A simple and accurate model to predict responses to multi-electrode stimulation in the retina. *PLOS Computat Biol,* 12(4):e1004849, 2016

[9] R.K. Shepherd, M.N. Shivdasani, D.A. Nayagam, C.E. Williams and P.J. Blamey. Visual prostheses for the blind, *Cell*, 31: 562571, 2013.

[10] K. Stingl et al. Artificial vision with wirelessly powered subretinal electronic implant alpha-IMS. *Proc Roy Soc B Biol Sci,* 280(1757): 20130077, 2013.

[11] W. Sun, N. Li, S. He. Large-scale morophological survey of rat retinal ganglion cells. *Vis Neurosci*, 19: 483493, 2002.